Postfire reliability analysis of axial load bearing capacity of CFRP retrofitted concrete columns

Bin Cai[1,2], Liyan Hao[1] and Feng Fu[*2]

[1]*School of Civil Engineering, Jilin Jianzhu University, Changchun, China*
[2]*School of Mathematics, Computer Science and Engineering, City, University of London, London, UK*

Abstract. A reliability analysis of the axial compressive load bearing capacity of postfire reinforced concrete (RC) columns strengthened with carbon fiber reinforced polymer (CFRP) sheets was presented. A 3D finite element (FE) model was built for heat transfer analysis using software ABAQUS. Based on the temperature distribution obtained from the FE analysis, the residual axial compressive load bearing capacity of RC columns was worked out using the section method. Formulas for calculating the residual axial compressive load bearing capacity of the columns after fire exposure and the axial compressive load bearing capacity of postfire columns retrofitted with CFRP sheets were developed. Then the Monte Carlo method was used to analyze the reliability of the axial compressive load bearing capacity of the RC columns retrofitted with CFRP sheets using a code developed in MATLAB. The effects of fire exposure time, load ratio, number of CFRP layers, concrete cover thickness, and longitudinal reinforcement ratio on the reliability of the axial compressive load bearing capacity of the columns after fire were investigated. The results show that within 60 minutes of fire exposure time, the reliability index of the RC columns after retrofitting with two layers of CFRPs can meet the requirements of Chinese code GB 50068 (GB 2001) for safety level II. This method is effective and accurate for the reliability analysis of the axial load bearing capacity of postfire reinforced concrete columns retrofitted with CFRP.

Keywords: CFRP; axial compressive capacity; postfire; reliability; Monte Carlo method

1. Introduction

Fire is a high-frequency disaster. High temperature influences the behavior of concrete at different structural levels (Zhang *et al*. 2014), and the mechanical properties of building materials vary greatly. Also, the load bearing capacity of reinforced concrete structures is significantly reduced (Wu 2014). To reduce the economic loss and ensure a structure's normal use after fire exposure, the reinforced concrete structure must be repaired and strengthened after fire. The fiber cloth affixation reinforcement method uses a matching adhesive to adhere fiber cloth to the concrete surface to achieve structural reinforcement and seismic strengthening. Compared with other reinforcement methods, affixing fiber-reinforced composite materials, especially carbon fiber reinforced polymer (CFRP) to concrete components has the advantages of high strength, high efficiency, easy construction, light weight, low cost, strong corrosion resistance and durability, suitability for a wide range of applications, low potential for damage to the strengthening components, and an almost perfect bonding with the structural components (Yue *et al*. 1998). Especially its postfire residual mechanical properties is of great concern (Shaikh and Taweel 2015). These fiber materials are relatively new but have been widely used in recent years

to reinforce concrete structures after fire exposure (Alsaad and Hassan 2017, Täljsten and Elfgren 2000, Yue 2000, Sen *et al*. 2001, Danilov *et al*. 2016) and have become a main topic of building material research, yielding a considerable volume of results.

To date, extensive research on the carbon fiber reinforcement of reinforced concrete columns after fire exposure has been conducted worldwide. Li *et al*. (2011) verified the effectiveness of CFRP sheets in strengthening reinforced concrete columns after fire. Alsayed *et al*. (2014) introduced the compressive properties of a wall-shaped rectangular RC column strengthened with CFRP. Abdel *et al*. (2015) concluded that the protective material had low thermal conductivity and good performance in fire, and the CFRP material used with an appropriate fireproof insulating material could withstand a high temperature for more than 70 minutes under a working load. Won *et al*. (2014) analyzed the fire resistance of internally confined hollow (ICH) reinforced concrete columns under ISO 834 standard fires and other certain initial conditions. Besides, the effects of various factors on fire resistance were analyzed. Sahamitmongkol *et al*. (2011) studied the damage of reinforced concrete columns under long-term high temperature through detailed inspection and finite element analysis. Alhatmey *et al*. (2018) analyzed the effects of the diameter-to-thickness ratio and reinforcing bars on the residual load bearing capacity, ductility and stiffness of concrete-filled steel tube stub columns after fire. Cree *et al*. (2012) studied the fire performance of circular and square reinforced concrete columns, and validated the numerical

---

∗Corresponding author, Associate Professor
 E-mail: cenffu@yahoo.co.uk

model developed specifically for cylindrical and square columns. Yazdani *et al*. (2018) used external CFRP laminates to establish a nonlinear theoretical model for the axially loaded concrete columns. Imran *et al*. (2018) established a heat transfer finite element model in ABAQUS and proposed a method for determining the fire resistance grade of the insulated columns strengthened with CFRP. Kim *et al*. (2014) proposed a numerical method to estimate the thermal conductivity of RC columns after fire exposure for design purpose. Winful *et al*. (2018) established a numerical model considering geometrical imperfections and material non-linearity in ABAQUS and validated the experimental data on high strength steel (HSS) at ambient temperature and low carbon steel at elevated temperatures. Doran *et al*. (2015) established a strength-enhancing model for the CFRP-constrained RC columns by a new artificial intelligence-based algorithm (Mamdani-type fuzzy inference system). Kodur *et al*. (2013) proposed a practical calculation method and formula for the load bearing capacity of steel reinforced concrete columns after fire. Xu (2010) studied the residual load bearing capacity of RC columns and the practical calculation method for determining the residual load bearing capacity of square columns after an ISO 834 standard fire. Some research results have been obtained by using CFRP sheets to strengthen concrete columns after fire exposure, but the research on its reliability is still insufficient. The reliability analysis of the axial compressive load bearing capacity of postfire reinforced concrete columns strengthened with CFRP has not been reported.

The columns are one of the most critical elements of a structure, and the investigation of the durability on the columns is crucial to the assessment of a building after fire exposure (Ada *et al*. 2018). As a widely used high-efficiency structural reinforcement material, CFRP can significantly improve the axial compressive capacity of RC columns after fire, and generally, the structure can still be reused when being repaired and reinforced after fire damage. Although the residual strength may meet the strength design requirements, it is still unclear whether the post-reinforced column has sufficient reliability for a further use. There still exists a high scatter and variability affecting the reliability of the structure (Gjørv 2013), such as the uncertainty of the performance of reinforced concrete after fire, the variability of the load, the uncertainty of the geometric parameters of the components and the uncertainty of the calculation model. To fill this gap, a framework developed by Cai *et al*. (2019) is used for the reliability analysis of the axial compressive load bearing capacity of postfire reinforced concrete columns strengthened with CFRP. The effects of various factors such as fire exposure time, concrete cover thickness, longitudinal reinforcement ratio and number of CFRP layers on the reliability of the axial compressive load bearing capacity of RC columns are investigated. The reliability numerical results and the parameter analysis after reinforcement have data guidance for practical engineering applications. The method developed in this paper can be used to evaluate the reliability of the axial load bearing capacity of reinforced concrete columns after fire exposure, which provides a

theoretical basis for the reinforcement and repair of damaged components after fire, and has practical significance.

2. Axial compressive strength calculation method for postfire RC columns

The temperatures at individual points in the section after fire exposure are different, and the mechanical properties of the components are also different. To accurately quantify the changes in the axial compressive strength of RC columns after fire exposure, a strength reduction calculation method is proposed. The numerical calculation model is established according to the following procedure.

2.1 Heat transfer analysis

The temperature distribution of the RC columns is determined through heat transfer analysis (Fu 2015，2016a, 2018).The finite element analysis software ABAQUS. Similar modelling techniques if (Fu 2008, 2010, 2012, Weng *et al*. 2020，Gao 2017, Qian 2020) is used to simulate RC columns during fire exposure.

2.1.1 Thermal parameters of materials
Severe exposure conditions such as fire and high temperatures can adversely affect the microstructure of the material, greatly reducing the strength of the structure. When the temperature is extremely high, the physical and chemical structure of the material has undergone substantial changes (Ahmad *et al*. 2018). Therefore, the thermal parameters of the material are the basic elements before the temperature field simulation, include the specific heat capacity and heat conductivity. The thermal parameters proposed in EN 1994-1-2 (BS 2013) are adopted in this paper.

The heat conductivity of concrete, λ_c, is given as

$$\lambda_c = 2 - 0.24\left(\frac{T}{120}\right) + 0.012\left(\frac{T}{120}\right)^2 \quad 20°C \leq T \leq 1200°C \quad (1)$$

The specific heat capacity of concrete, C_c, is given as

$$C_c = 900 - 4\left(\frac{T}{120}\right)^2 + 80\left(\frac{T}{120}\right) \quad 20°C \leq T \leq 1200°C \quad (2)$$

The heat conductivity of steel bars, λ_s, is given as

$$\lambda_s = 54 - 3.33 \times 10^{-2}T \quad 20°C \leq T \leq 800°C \quad (3)$$
$$\lambda_s = 27.3 \quad\quad\quad 800°C < T \leq 1200°C \quad (4)$$

The specific heat capacity of steel bars, C_s, is given as

$$C_s = 425 + 7.73 \times 10^{-1}T - 1.69 \times 10^{-3}T^2 + 2.22 \times 10^{-6}T^3$$
$$20°C \leq T < 600°C \quad (5)$$

$$C_s = 666 + \frac{13002}{738 - T} \quad\quad 600°C \leq T < 735°C \quad (6)$$

$$C_s = 545 + \frac{17820}{T - 731} \quad\quad 735°C \leq T < 900°C \quad (7)$$

$$C_s = 65 \quad\quad\quad\quad 900°C \leq T < 1200°C \quad (8)$$

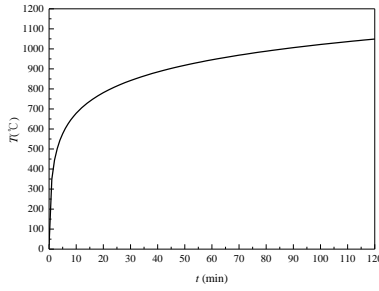The heating curve adopts the ISO 834 standard fire temperature curve (ISO 1999) defined by the equation

Fig. 1 ISO 834 standard fire curve

Fig. 2 Temperature distribution of the column section after fire exposure

below, also as shown in Fig. 1

$$T = T_0 + 345 \lg(8t+1) \quad (9)$$

where T_0 is room temperature and t is the heating time.

2.1.2 Temperature field using ABAQUS

The finite element analysis software ABAQUS is used to simulate the temperature field of the components of the columns. The thermal parameters of the material are determined by Eqs. (1)-(8), the heating curve is determined by Eq. (9), and a finite element model of RC columns with different fire durations is established for a temperature field analysis. The concrete is simulated by a three-dimensional solid heat conduction element (DC3D8), and the steel is modeled with a DC1D2 heat-conducting connection element (Wang *et al.* 2016). The element is assumed to have isotropic material properties, and its surface can exchange energy with the outside by thermal convection and heat radiation. The influence of thermal resistance between steel and concrete on the temperature field is ignored, so tie contacts are used between steel and concrete.

2.2 A modified formula to calculate the residual axial compressive load bearing capacity of the column after fire exposure

After fire exposure, degradation of mechanical properties of steel bars and concrete leads to a reduction in the axial load bearing capacity and further affects the safety of the columns (Guo *et al.* 2003, Fu 2016b). Before the reliability evaluation of columns subjected to fire, it is necessary to conduct a quantitative analysis of the capacity attenuation of each component. Based on the result of heat transferring analysis using finite element program ABAQUS, a material strength reduction formula from Chinese code GB 50153 (GB 2008) is introduced to determine the residual strengths of the materials after fire, and the residual axial load bearing capacity of postfire RC columns is subsequently determined.

2.2.1 Determining the material strength degradation after fire exposure

After fire exposure, the strengths of reinforcement and concrete decrease. According to GB 50153 Unified Standards for Reliability Design of Engineering Structures (GB 2008), the reduction coefficient of the compressive strength of concrete after fire, φ_{cT} is given as
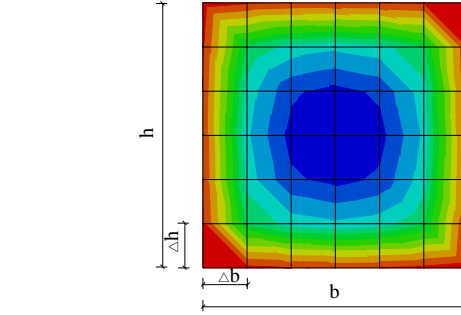
$$\varphi_{cT} = \frac{f_{cr}(T)}{f_c} = \begin{cases} 1.0 & 0°C < T \leq 200°C \\ 1.0 - 0.0015(T-200) & 200°C < T \leq 500°C \\ 0.25 + 0.003(600-T) & 500°C < T \leq 600°C \\ 0.25 - 7.5 \times 10^{-4}(T-600) & 600°C < T \leq 800°C \end{cases} \quad (10)$$

where $f_{cr}(T)$ is the axial compressive strength of concrete at $T°C$ after fire and f_c is the axial compressive strength at room temperature.

The yield strength reduction factor (Shen 1991) of steel after fire, φ_{yT}, is given as

$$\varphi_{yT} = \frac{f_{yr}(T)}{f_y} = \begin{cases} (99.838 - 0.0156T) \times 10^{-2} & 0°C < T < 600°C \\ (137.35 - 0.0754T) \times 10^{-2} & 600°C \leq T \leq 900°C \end{cases} \quad (11)$$

where $f_{yr}(T)$ is the yield strength of steel at $T°C$ after fire and f_y is the yield strength of steel at room temperature.

2.2.2 Calculating the residual axial compressive strength after fire exposure

After the temperature distributions and the postfire material strength reduction factor were determined, the residual axial compressive strength could be determined using the section method of existing literatures (EI-Fitiany and Youssef 2017). The method is based on the following basic assumptions:

1. There are differences in the concrete strength for different units in the compression zone, but the strength in each small unit is regarded as constant after fire;

2. The equivalent reduction coefficient of the concrete strength in the entire compression zone can be obtained by taking a weighted average over the area of the compression zone;

3. The effect of temperature stress on the strength of the concrete at high temperature is not considered.

The temperature distribution after fire is determined according to Section 2.1, and the material strength reduction factor after fire is determined according to Section 2.2.1. A section of the column after fire exposure is divided as shown below (Fig. 2).

The average strength reduction factor of concrete in the compression zone of the component is given by

$$\bar{\varphi}_{cT} = \frac{\sum \varphi_{cT_i} f_c \Delta b \Delta h}{f_c bh} \quad (12)$$

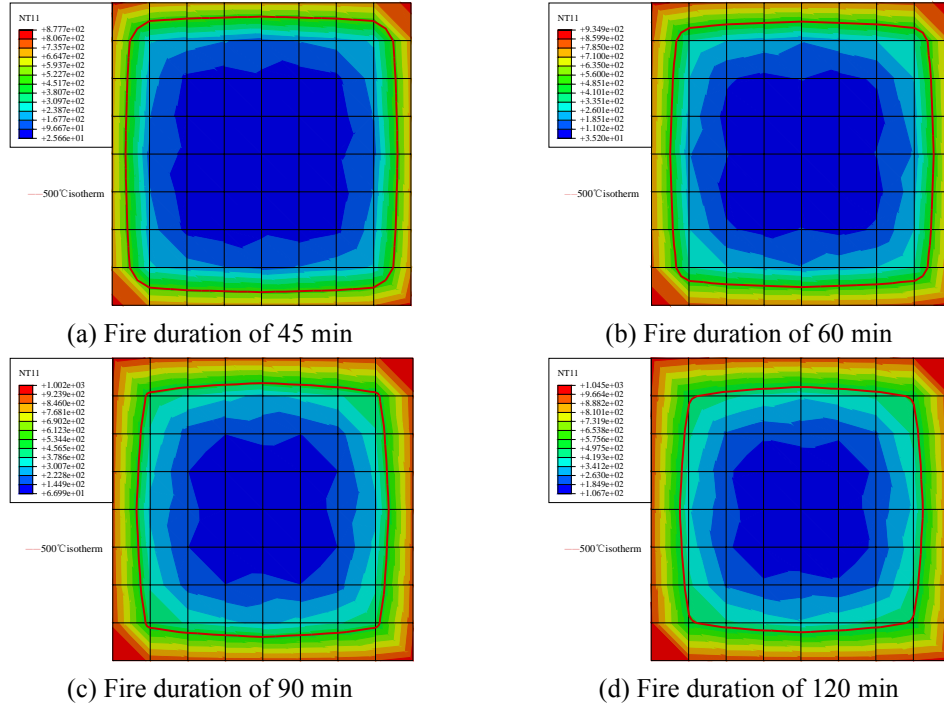where b is the column cross-section width, h is the cross-

(a) Fire duration of 45 min   (b) Fire duration of 60 min

(c) Fire duration of 90 min   (d) Fire duration of 120 min

Fig. 3 Temperature distributions within the column cross-section for different fire durations (unit: °C)

section depth and φ_{cT_i} is the concrete compressive strength reduction factor in the *i*th region, which is calculated from the highest temperature (T_i) experienced in the *i*th region and Eq. (10). Considering that the strength reduction after fire is only related to the maximum temperature of the fire, the calculation of the axial load bearing capacity can be carried out after the highest temperature field of the interface is obtained.

Before fire exposure, according to GB 50010 Code for Design of Concrete Structures (GB 2010), the normal load bearing capacity of an axially compressed column is given by

$$N_c = 0.9\varphi(f_c A + f'_y A_s) \tag{13}$$

where φ is the stability coefficient which is mainly related to the component's slenderness ratio, A is the cross-sectional area of the column, f'_y is the yield strength of the compression rebars at room temperature, and A_s is the total area of cross-section of the compression rebars.

The attenuation of the bearing capacities of structural members after fire is mainly reflected in the material properties. The reduction trend of the component's load bearing capacity is basically consistent with the strength reduction trends of concrete and steel bar (Xu *et al*. 2013, Chen *et al*. 2018). Based on Eq. (13), a modified formula to calculate the residual axial compressive strength of RC columns after fire exposure is developed by the authors below through the consideration of the thermal effect

$$N_{cT} = 0.9\varphi[\bar{\varphi}_{cT} f_c A + \varphi'_{yT} f'_y A_s] \tag{14}$$

where N_{cT} is the axial compressive capacity of the RC column at T°C after fire and φ'_{yT} is the yield strength reduction factor of the compressive reinforcement.

2.2.3 Validation of the calculation method

The test results by Xu (2010) for the residual load bearing capacity of reinforced concrete columns after fire exposure were selected for comparison and verification. In his test, after fire duration of 45, 60, 90 and 120 min, the residual load bearing capacities of the axially loaded square columns were 4797.8 kN, 4494.1 kN, 3868.8 kN and 3491.7 kN, respectively.

The 500°C isotherm method for concrete in Eurocode 2 Part 1-2 (BSI 2004) considers the difference in the mechanical properties of materials caused by an uneven temperature distribution within the section (Lie 1992). The method comprises a general reduction of the cross-section size with respect to a heat damaged zone at the concrete surfaces. The thickness of the damaged concrete is made equal to the average depth of the 500°C isotherm in the compression zone of the cross-section. The damaged concrete with temperature in excess of 500°C, is assumed not to contribute to the load bearing capacity of the member, whilst the residual concrete cross-section retains its initial strength, which changes an uneven temperature field within the cross section at high temperature to a uniform temperature field. Using this method to simulate the temperature field of Xu's case and calculate the residual capacity, the errors between the obtained results and Xu's experimental results were 9.1%, 10.9%, 14.8% and 22.8%, respectively.

Based on the simulation method used in this paper, the component's temperature field is simulated according to Xu's actual experimental conditions, and the temperature distributions of reinforcement and concrete are shown in Figs. 3-4, NT11 is the temperature value, so Figs. 3-4 show the contours of the temperature across the section. The red line marked in Fig. 3 is the 500°C isotherm which is the

(a) Fire duration of 45 min   (b) Fire duration of 60 min

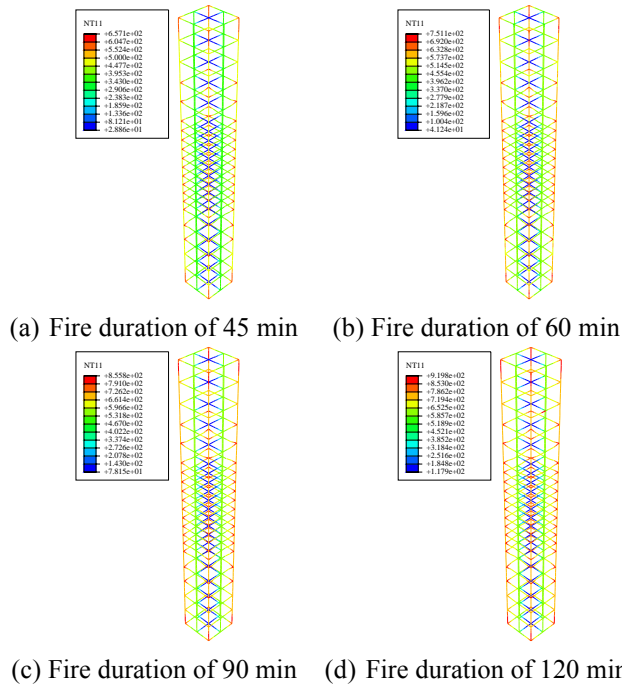(c) Fire duration of 90 min   (d) Fire duration of 120 min

Fig. 4 Temperature distributions within the reinforcement for different fire durations (unit: °C)

Table 1 Simulation verification results and comparison

		500°C isotherm method	Method in this paper	
	Actual value(kN)	Simulation value (kN)	Error	Simulation value (kN)	Error
45 min	4797.8	4361.5	9.10%	4741.1	1.18%
60 min	4494.1	4003.3	10.9%	4433.4	1.35%
90 min	3868.8	3294.2	14.8%	3939.0	1.81%
120 mn	3491.7	2693.8	22.8%	3560.3	1.96%

basis of the Eurocode 500°C isotherm method. The temperature distributions of reinforcement and concrete under different fire durations were extracted, and strength reduction calculations were performed to obtain the corresponding residual load-bearing capacities. As the results shown in Table 1 and compared with Xu's results, the errors are all within 2%, the precision is higher, and the fitting effect is better. In contrast with the 500°C isotherm method, this method of simulating the temperature field and calculating the load bearing capacity is more feasible, and the following calculations of reliability can be performed.

3. Reliability analysis

3.1 Reliability calculation based on the Monte Carlo method

The Monte Carlo method (Cardoso *et al*. 2008) is also called the random sampling method. This method simulates a large number of mathematical statistical experiments. The simulated eigenvalues are used as the numerical solution of the problem. The accuracy of the solution is directly affected by the number of samples. According to the
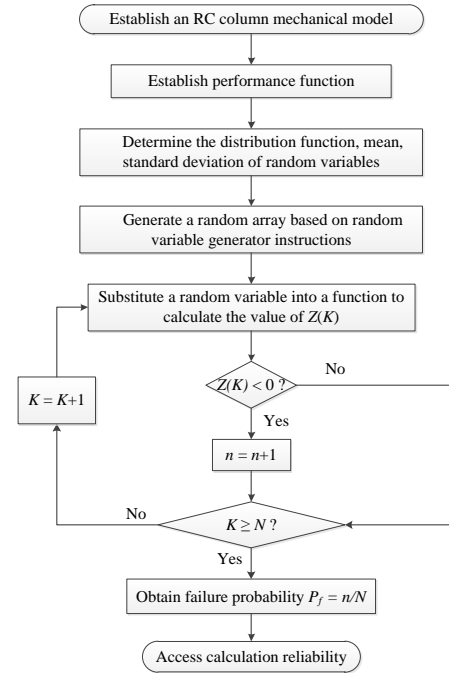

Fig. 5 Reliability calculation flow chart of Monte Carlo Method

principle of the Monte Carlo method, combined with the limit state function of axial compressive capacity of reinforced concrete columns and the probability model of random variables, 10^6 simulation cycles were performed by MATLAB, and the reliability was accurately calculated.

The effects of concrete cover thickness, longitudinal reinforcement ratio, load ratio and carbon fiber usage on the reliability index of the axially compressive capacity of columns retrofitted with CFRP sheets after fire exposure are studied. The flow chart for calculating the reliability index by Monte Carlo method (Feng and Yang 2002) is as follows in Fig. 5.

3.2 RC column design

For a structural design and reliability analysis, load combinations must be considered for various loads that the structure may withstand during its design life, such as static loads, roof live loads, snow loads, wind loads and seismic loads, etc. When performing a reliability analysis under fire conditions, Ellingwood (2005) focused on the frequency analysis of these loads and fire simultaneously but neglected the possibility of the simultaneous occurrence of fire and extreme loads including snow, earthquakes, wind, etc. Therefore, in this study, fire is only considered in combination with a static load and a continuous live load.

For an RC column in an ultimate state, its axial compressive load bearing capacity at room temperature should satisfy

$$N_{Sd} \leq N_{Rd} \tag{15}$$

where N_{Sd} is the design value of the axial load, and N_{Rd} is the design value of the component's axial resistance.

The axial design load should be calculated according to the design value with the most unfavorable effect (GB2012)

Table 2 Statistical parameters of design variables

Variable	Physical meaning	Distribution	Bias (mean)	CoV (std)
f_c (N/mm^2)	C30 compressive strength	log-normal	1.395	0.172
f_y (N/mm^2)	HRB400 steel yield stress	log-normal	1.156	0.082
N_Q (kN/m^2)	live load	extreme type I	0.859	0.233
N_G (kN/m^2)	dead load	normal	1.060	0.070
γ_m	total model uncertainty	normal	1	0.025
b (mm)	column width	normal	1	0.01
h (mm)	column depth	normal	1	0.01
f_f (MPa)	CFRP tensile strength	Weibull	1.152	0.08
t_f (mm)	CFRP strip thickness	log-normal	1	0.01
$\bar{\varphi}_{cT}$	T°C concrete compressive strength reduction factor	Beta	temperature-dependent conforming to EN 1992-1-2	temperature-dependent
φ'_{yT}	T°C reinforcement yield strength reduction factor	Beta	temperature-dependent conforming to EN 1992-1-2	temperature-dependent

Note: Bias is the mean value/nominal value, CoV is the coefficient of variation and std is the standard deviation

$$N_{Sd} = \max\left\{(\xi\gamma_G N_{Gk} + \gamma_Q N_{Qk}); (\gamma_G N_{Gk} + \gamma_Q \psi_c N_{Qk})\right\} \quad (16)$$

where ξ is the reduction factor for a constant dead load, γ_G is the partial coefficient for dead load, N_{Gk} is the standard value of the axial force (N_G) generated by the dead load, N_{Qk} is the standard value of the axial force (N_Q) generated by the live load, γ_Q is the partial coefficient for live load, and ψ_c is the combination value adjustment factor for the live load. The values for N_{Gk} and N_{Qk} of the components are determined by

$$N_{Gk} = \frac{N_{Rd}}{\max\left\{(\xi\gamma_G + \gamma_Q \frac{N_{Qk}}{N_{Gk}}); (\gamma_G + \gamma_Q \psi_c \frac{N_{Qk}}{N_{Gk}})\right\}} \quad (17)$$

$$N_{Qk} = k N_{Gk} \quad (18)$$

where k is the ratio of the live load to the dead load, and the N_{Sd} value is calculated from Eq. (16) to design the reinforcement.

In this case, the cross-sectional dimensions of the axially compressed reinforced concrete columns are designed as $b \times h = 300$ mm$\times$300 mm, the calculated height L is 4550 mm, $\varphi = 0.8908$, the concrete grade is C30, the concrete cover c is 25 mm, the longitudinal reinforcement is HRB400, four compression-bearing rebars with diameters of 25 mm are configured and the stirrups are made of HRB335, with a diameter of 8 mm and a spacing of 200 mm.

3.3 Limit state equation

Maximum structural load bearing capacity relates to structural failure mode (Zhou 2019). In the structural reliability analysis, a limit state function can be established below to describe whether the structure can perform the predetermined function (Gong and Wei 2007)

$$Z = R - S = g\left(X_1, X_2, ... X_n\right) \quad (19)$$

where $g(x)$ is the failure function, X_1, X_2, ..., X_n are n independent random variables, R is the resistance of the structure, and S is the effect of the structure. When $Z>0$, the

structure is in a reliable state, when $Z<0$, the structure is in a failure state, and when $Z=0$, the structure is in a limit state.

When calculating the axial compressive strength of RC columns, the basic assumptions used in the calculation can not completely match the actual values, and the approximate value of the calculated result will cause variability in the calculated load bearing capacity. Therefore, a random variable is introduced: the uncertainty coefficient of structural resistance calculation mode, γ_m.

The performance function of the axially compressed column prior to reinforcement is given as

$$Z = R - S = \gamma_m \cdot N_c - (N_G + N_Q) \quad (20)$$

The performance function of the axially compressed column after fire exposure is given as

$$Z = R - S = \gamma_m \cdot N_{cT} - (N_G + N_Q) \quad (21)$$

The reduced axial compressive load bearing capacity of RC columns after fire exposure can be strengthened by using CFRPs. The formula to calculate the axial compressive load bearing capacity of retrofitted columns after fire is developed by the authors based on GB 50367 Code for Design of Strengthening Concrete Structure (GB 2013) through the inclusion of the thermal effect. The circumferential confinement method for load-bearing capacity is further modified as follows

$$N_d = 0.9\left[(\bar{\varphi}_{cT} f_c + 4\sigma_t)A_{cor} + \varphi'_{yT} f'_y A_s\right] \quad (22)$$

$$\sigma_t = 0.5\beta_c k_c \rho_f E_f \varepsilon_{fe} \quad (23)$$

where σ_t is the effective constraint stress, A_{cor} is the area of the concrete inside the circumferential confinement, β_c is the influence coefficient of concrete strength, k_c is the effective constraint factor of the circumferential confinement, ρ_f is the circumferential confinement volume ratio, E_f is the elastic modulus of the carbon fiber, and ε_{fe} is the effective tensile strain of the carbon fiber.

Therefore, the performance function of an axially compressed column strengthened with CFRP after fire exposure is
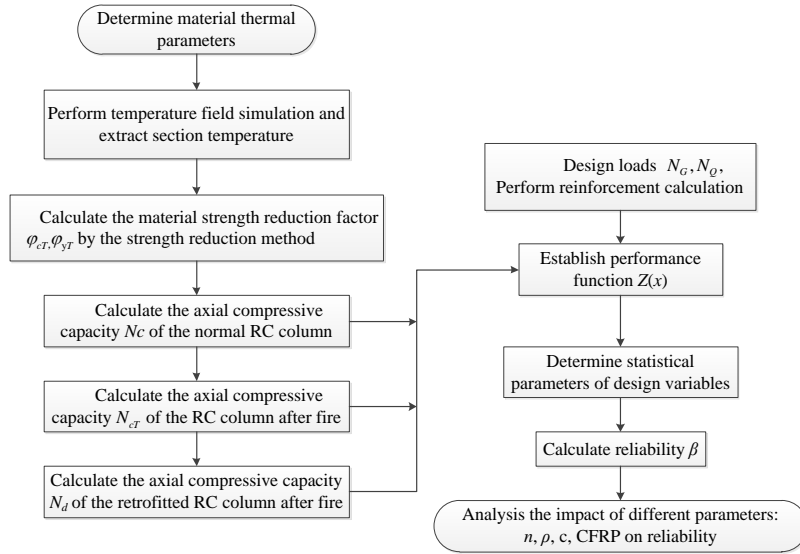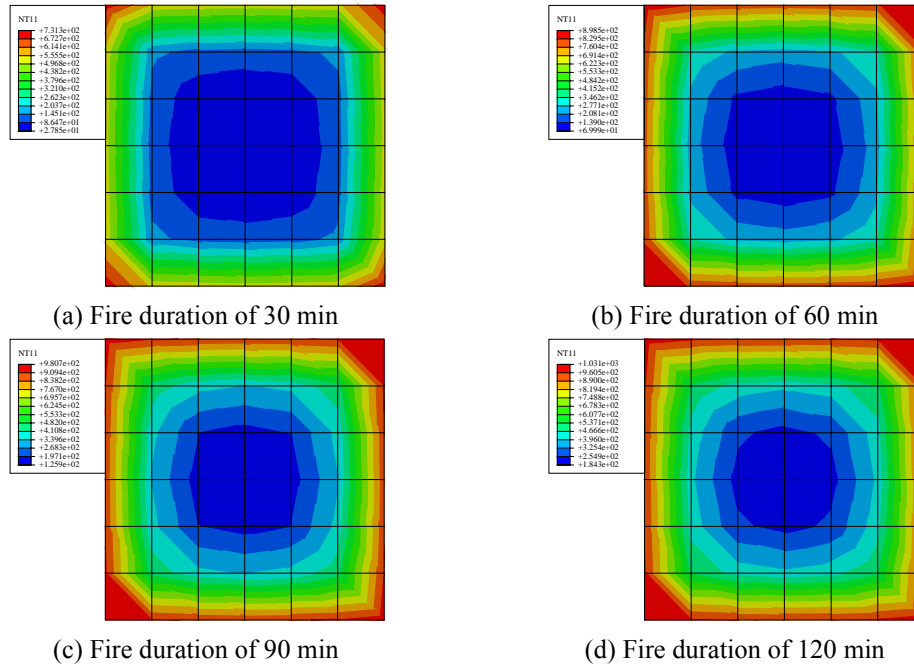
Fig. 6 Flow chart for calculation

(a) Fire duration of 30 min

(b) Fire duration of 60 min

(c) Fire duration of 90 min

(d) Fire duration of 120 min

Fig. 7 Column cross-section temperature field distributions for different fire durations (unit: °C)

$$Z = R - S = \gamma_m \cdot N_d - (N_G + N_Q) \tag{24}$$

3.4 Statistical parameters of design variables

In this paper, the Monte Carlo method is used to calculate the reliability index of axially compressed RC columns before and after fire exposure and strengthening. The statistical parameters of random variables used in the MATLAB data analysis (Cai 2016, 2018, Van Coile 2013, 2017) are shown in Table 2.

In order to discuss the difference in reliability between different load values for the design case (Gong 2000), the load ratio n is introduced as $n=N_Q/N_G$, where n takes values from 0.1 to 2 (Yuan 2017) in general.

4. Case study and reliability analysis for different parameters

In this section, the case study for RC column after fire is performed.

4.1 Calculation process

The flow chart in Fig. 6 provides a detailed overview of the steps required to apply the postfire strength reduction method and subsequent reliability analysis of RC columns.

4.2 Heat transfer simulation

In ABAQUS, the heating curve is based on the ISO 834 standard heating curve. The specific heat capacity, thermal
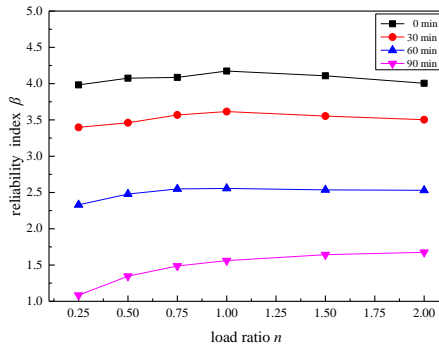
Fig. 8 Reliability index versus load ratios for different fire durations

Fig. 9 Reliability index versus fire duration for different reinforcement ratios

conductivity and mass density of concrete are calculated based on the formula given by EN1994 Part 1-2 (BSI 2013). The mesh size of the cross-section is divided into 50 mm, which can meet the accuracy requirements. The temperature field distributions of the column cross-section at fire durations of 30, 60, 90 and 120 min are shown in Fig. 7. The average temperature of the concrete and reinforcement for any in-fire duration can be calculated.

4.3 Reliability analysis for different parameters

The factors affecting the reliability index of postfire RC columns include the concrete cover thickness, longitudinal reinforcement ratio, load ratio, fire duration, and the number of CFRP layers. The Monte Carlo method is applied to obtain the reliability index of the axial compressive capacity of RC columns after fire. The load ratio ranges from 0.25 to 2, the concrete cover thicknesses are 25 mm and 35 mm, the reinforcement ratios are 1.69%, 2.18%, and 2.53%, and the fire duration varies from 0 to 120 minutes. The influences of various factors on the reliability of RC columns are analyzed.

4.3.1 Effects of Load ratio

Fig. 8 indicates the reliability curves of RC columns under different load ratios as a function of fire duration. The concrete cover thickness is 25 mm, and four compression rebars with a diameter of 25 mm are configured. The load ratio n was set to 0.25, 0.50, 0.75, 1.00, 1.50 and 2.00.

Fig. 8 indicates that the reliability index β is significantly reduced after fire exposure, and the load ratio has an impact on the reliability index. Further analysis shows that when the load ratio changes from 0.25 to 1, the reliability index increases with the increase in the load ratio. This is mainly because within a certain range, the contribution of the live load to the combined load effect increases. Compared with the dead load, the coefficient of variation δ and the load partial coefficient γ of the live load are larger. As the load ratio increases, γ causes β to increase and δ causes β to decrease, but γ has a more significant effect. Therefore, the reliability index significantly changes with the increase in the load ratio. Beyond a certain range, though δ gradually begins to play a more important role, there is a growth balance in reliability index and the change is not as obvious.
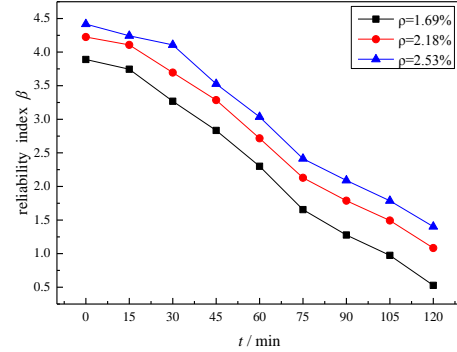
4.3.2 Effects of Longitudinal reinforcement ratio

Fig. 9 shows the reliability curves of RC columns under different longitudinal reinforcement ratios as a function of the fire duration. The concrete cover thickness is 25 mm, and four compression rebars with diameters of 22 mm and 25 mm and six compression rebars with diameters of 22 mm are configured, respectively. The reinforcement ratios are 1.69%, 2.18% and 2.53%, correspondingly, and the load ratio is n=1.

Fig. 9 shows that the reliability index increases with the reinforcement ratio within the range that meets the reinforcement ratio requirements. The influence degree of reinforcement ratio on the reliability decreases as the reinforcement ratio increases. This is mainly because the increase in reinforcement ratio reduces the variability of column resistance.

4.3.3 Effects of number of CFRP layers and cover thickness

There are many ways to enhance the load bearing capacity of an axially compressed column. In this case, CFRP sheets are placed continuously along the entire circumference without a gap (referred to as the circumferential confinement method) to strengthen RC columns after fire damage. The CFRP tensile strength (f_f) is 3 000 MPa, the elastic modulus (E_f) is 230 GPa, the thickness of a single layer (t_f) is 0.111 mm, the corner radius (r) is 20 mm, and the safety class is II. The material parameters are shown in Table 2.

Figs. 10-11 show the reliability curves of RC columns for different layers of CFRP as a function of the fire duration. The concrete cover thickness is 25 mm in Fig. 10 and 35 mm in Fig. 11. Four compression rebars with diameters of 25 mm are configured. The load ratio is n = 1. The reliability is calculated for fire duration from 30 to 120 min.

A comparison of Figs. 10-11 shows that the reliability index increases with the concrete cover thickness. The longer the fire duration is, the greater influence of the concrete cover thickness reflects on the reliability. This is mainly because the increase in the concrete cover thickness delays the increase in the temperature of the steel and alleviates the deterioration of the steel's mechanical properties. It can be seen from Figs. 9-10 that, under the same conditions, the reliability index increases more
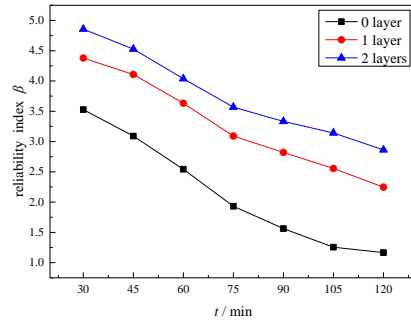
Fig. 10 Reliability index versus fire duration for different layers of CFRP when *c*=25 mm

Fig. 11 Reliability index versus fire duration for different layers of CFRP when *c*=35 mm

significantly with more CFRP layers, even a single reinforcement layer may result in a significant improvement of reliability index. Within 60 min of fire duration, after strengthening two layers of CFRP, the RC column can meet the requirements of specification GB 50068 (GB 2001) for the reliability index of brittle components with safety class II being greater than 3.7.

5. Conclusions

In this paper, a reliability analysis method for the axial compressive load bearing capacity of the postfire RC columns retrofitted with CFRP sheets is proposed. The load ratio, fire exposure time, concrete cover thickness, longitudinal reinforcement ratio and number of CFRP layers are considered in the process of reliability analysis. After analysis, the following conclusions are obtained:

• The results obtained from the calculation method of the axial load bearing capacity after fire exposure agree well with the experimental results in the referenced literature. The method proposed in this paper has a higher accuracy compared with the 500°C isotherm method and thus can be applied in engineering practice. The reliability model can quickly and accurately calculate the reliability of the axial compressive load bearing capacity of postfire RC columns.

• The reliability index of the axial compressive load bearing capacity of the reinforced concrete columns increases first and then becomes gentler with the increase in the load ratio but decreases sharply with the increase in fire duration.

• As the concrete cover thickness increases, the reliability index of RC columns increases. The concrete cover has a significant impact on the reliability of the axial compressive load bearing capacity of RC columns after fire.

• As the longitudinal reinforcement ratio increases, the reliability index increases. Increasing the reinforcement ratio can effectively improve the reliability of the column.

• With the increase in the CFRP reinforcement thickness, the reliability index obviously increases, and strengthening with two layers of CFRP results in a significant improvement in the reliability index of reinforced concrete columns for the axial compressive
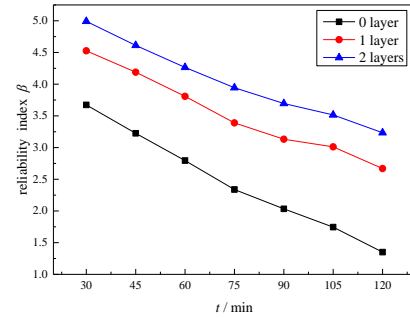
strength, which provides a reasonable method for strengthening and improving the reliability of damaged components after fire.

Reference

Abdel-Hafez, L.M., Abouelezz, A.E.Y. and Hassan, A.M. (2015), "Behavior of RC columns retrofitted with CFRP exposed to fire under axial load", *HBRC J.*, **11**(1), 68-81. https://doi.org/10.1016/j.hbrcj.2014.02.002.

Ada, M., Sevim, B., Yüzer, N. and Ayvaz, Y. (2018), "Assessment of damages on a RC building after a big fire", *Adv. Concrete Constr.*, **6**(2), 177-197. http://dx.doi.org/10.12989/acc.2018.6.2.177.

Ahmad, H., Hameed, R., Riaz, M.R. and Gillani, A.A. (2018), "Strengthening of concrete damaged by mechanical loading and elevated temperature", *Adv. Concrete Constr.*, **6**(6), 645-658. http://dx.doi.org/10.12989/acc.2018.6.6.645.

Alhatmey, I.A., Ekmekyapar, T. and Alrebeh, S.K. (2018), "Residual strength capacity of fire-exposed circular concrete-filled steel tube stub columns", *Adv. Concrete Constr.*, **6**(5), 485-507. http://dx.doi.org/10.12989/acc.2018.6.5.485.

Alsaad, A. and Hassan, G. (2017), "Utilization of CFRP for strengthening RC columns in marine environment", *Case Stud. Constr. Mater.*, **7**, 30-35. https://doi.org/10.1016/j.cscm.2017.05.002.

Alsayed, S.H., Almusallam, T.H., Ibrahim, S.M., Al-Hazmi, N.M., Al-Salloum, Y.A. and Abbas, H. (2014), "Experimental and numerical investigation for compression response of CFRP strengthened shape modified wall-like RC column", *Constr. Build. Mater.*, **63**, 72-80. https://doi.org/10.1016/j.conbuildmat.2014.04.047.

BSI (2004), Eurocode 2 - Design of Concrete Structures-Part 1-2: General Rules-Structural fire Design, British Standards Institution, London, UK.

BSI (2013), Eurocode 4-Design of Composite Steel and Concrete Structures-Part 1-2: General Rules-Structural Fire Design,

British Standards Institution, London, UK.

Cai, B. and Yuan, Y.H. (2016), "Reliability of bending capacity for corroded reinforced concrete beam strengthened with CFRP", *Concrete*, (10), 148-151.

Cai, B. and Zhao, L.L. (2018), "Research of reliability of bearing capacity for corroded axial-compression reinforced concrete column strengthened with CFRP", *Arch. Technol.*, **49**(1), 65-68.

Cai, B., Zhang, B. and Fu, F. (2019), "A new Reliability analysis approach of flexural capacity of post-fire reinforced concrete beams retrofitted with CFRPs", *Proceedings of the Institution of Civil Engineers: Structures and Buildings*, 1-15. https://doi.org/10.1680/jstbu.19.00037.

Cardoso, J.B., Almeida, J.R.D., Dias, J.M. and Coelho, P.G. (2008), "Structural reliability analysis using Monte Carlo simulation and neural networks", *Adv. Eng. Softw.*, **39**(6), 505-513. https://doi.org/10.1016/j.advengsoft.2007.03.015.

Chen, Z.P., Zhou, S.W. and Liang, H.R. (2018), "Shear behavior test and bearing capacity calculation of recycled aggregate concrete beam after high temperature", *J. Nat. Disast.*, **27**(5), 140-152. https://doi.org/10.1016/j.conbuildmat.2015.12.103.

Cree, D., Chowdhury, E.U., Green, M.F., Bisby, L.A. and Benichou, N. (2012), "Performance in fire of FRP-strengthened and insulated reinforced concrete columns", *Fire Saf. J.*, **54**, 86-95. https://doi.org/10.1016/j.firesaf.2012.08.006.

Danilov, A.I. (2016), "Some aspects of CFRP steel structures reinforcement in civil engineering", *Procedia Eng.*, **153**, 124-130. https://doi.org/10.1016/j.proeng.2016.08.091.

Doran, B., Yetilmezsoy, K. and Murtazaoglu, S. (2015), "Application of fuzzy logic approach in predicting the lateral confinement coefficient for RC columns wrapped with CFRP", *Eng. Struct.*, **88**, 74-91. https://doi.org/10.1016/j.engstruct.2015.01.039.

El-Fitiany, S.F. and Youssef, M.A. (2017), "Fire performance of reinforced concrete frames using sectional analysis", *Eng. Struct.*, **142**, 165-181. https://doi.org/10.1016/j.engstruct.2017.03.065.

Ellingwood, B.R. (2005), "Load combination requirements for fire-resistant structural design", *Fire Protect Eng.*, **15**(1), 43-61. https://doi.org/10.1177/1042391505045582.

Feng, X.B. and Yang, H. (2002), "Realization of structural reliability by Monte Carlo method with MATLAB", *China Rural Water Hydrop.*, **8**, 50-51.

Fu, F. (2012), "Response of a multi-storey steel composite building with concentric bracing under consecutive column removal scenarios", *J. Constr. Steel Res.*, **70**, 115-126. https://doi.org/10.1016/j.jcsr.2011.10.012.

Fu, F. (2015), *Advanced Modeling Techniques in Structural Design*, John Wiley & Sons, Ltd.

Fu, F. (2016a), *Structural Analysis and Design to Prevent Disproportionate Collapse*, CRC Press, Boca Raton, FL, USA.

Fu, F. (2016b), "3D finite element analysis of the whole-building behavior of tall building in fire", *Adv. Comput. Des.*, **1**(4), 329-344. http://dx.doi.org/10.12989/acd.2016.1.4.329.

Fu, F. (2018), *Design and Analysis of Tall and Complex Structures*, Elsevier, London, UK.

Fu, F., Lam, D. and Ye, J.Q. (2008), "Modelling semi-rigid composite joints with precast hollowcore slabs in hogging moment region", *J. Constr. Steel Res.*, **64**(12), 1408-1419. https://doi.org/10.1016/j.jcsr.2008.01.012.

Fu, F., Lam, D. and Ye, J.Q. (2010), "Moment resistance and rotation capacity of semi-rigid composite connections with precast hollowcore slabs", *Steel Constr.*, **66**(3), 452-461. https://doi.org/10.1016/j.jcsr.2009.10.016.

Gao, S., Guo, L., Fu, F. and Zhang, S. (2017), "Capacity of semi-rigid composite joints in accommodating column loss", *J. Constr. Steel Res.*, **139**, 288-301. https://doi.org/10.1016/j.jcsr.2017.09.029.

GB (2001), GB 50068-2001: Unified Standard for Reliability Design of Building Structures, China Architecture Industry Press, Beijing, China.

GB (2008), GB 50153-2008: Unified Standards for Reliability Design of Engineering Structures, China Architecture Industry Press, Beijing, China.

GB (2010), GB 50010-2010: Code for Design of Concrete Structures, China Architecture and Building Press, Beijing, China.

GB (2012), GB 50009-2012: Load Code for the Design of Building Structures, China Architecture and Building Press, Beijing, China.

GB (2013), GB 50367-2013: Code for Design of Strengthening Concrete Structure, China Architecture and Building Press, Beijing, China.

Gjørv, O.E. (2013), "Durability design and quality assurance of major concrete infrastructure", *Adv. Concrete Constr.*, **1**(1), 45-63. http://dx.doi.org/10.12989/acc.2013.1.1.045.

Gong, J.X. and Wei, W.W. (2007), *Design Principle of the Reliability of Engineering Structures*, China Machine Press, Beijing, China.

Gong, J.X., Zhao, G.F. and Liu, L. (2000), "Reliability analysis of reinforced concrete axially compressed members after rehabilitation", *Build. Struct.*, **30**(3), 29-33.

Guo, Z.H. and Shi, X.D. (2003), *Behaviour of Reinforced Concrete at Elevated Temperature and its Calculation*, Tsinghua University Press, Beijing, China.

Imran, M., Mahendran, M. and Keerthan, P. (2018), "Heat transfer modelling of CFRP strengthened and insulated steel tubular columns", *Constr. Build. Mater.*, **184**, 278-294. https://doi.org/10.1016/j.conbuildmat.2018.06.205.

ISO (International Organization for Standardization) (1999), ISO 834-1: Fire-Resistance Tests-Elements of Building Construction-Part 1: General Requirements, International Organization for Standardization, Geneva, Switzerland.

Kim, J.J., Youm, K.S. and Reda T.M.M. (2014), "Extracting concrete thermal characteristics from temperature time history of RC column exposed to standard fire", *Scientif. World J.*, **2014**, 1-10. https://doi.org/10.1155/2014/242806.

Kodur, V.K.R., Raut, N.K., Mao, X.Y. and Khaliq, W. (2013), "Simplified approach for evaluating residual strength of fire-exposed reinforced concrete columns", *Mater. Struct.*, **46**(2), 2059-2075. ttps://doi.org/10.1617/s11527-013-0036-2.

Li, J.H., Yu, C.H., Tang, Y.F., Liu, M.Z. and Xiao, H. (2011), "Experimental research on rehabilitation with CFRP sheets for reinforced concrete columns after exposure to fire", *J. Arch. Civil Eng.*, **28**(4), 48-54.

Lie, T.T., Rowe, T.J. and Lin, T.D. (1986), "Residual strength of fire-exposed reinforced concrete column", *Am. Concrete Inst.*, **92**, 153-174.

Qian, K., Liang, S.L., Xiong, X.Y., Fu, F. and Fang, Q. (2020), "Quasi-static and dynamic behavior of precast concrete frames with high performance dry connections subjected to loss of a penultimate column scenario", *Eng. Struct.*, **205**, 110115-110115. https://doi.org/10.1016/j.engstruct.2019.110115.

Sahamitmongkol, R., Choktaweekarn, P., Sancharoen, P. and Tangtermsirikul, S. (2011), "Damage analysis of an RC column subjected to long-term transient elevated temperature", *Struct. Infrastr. Eng.*, **7**(12), 921-930. https://doi.org/10.1080/15732470903241873.

Sen, R., Liby, L. and Mullins, G. (2001), "Strengthening steel bridge sections using CFRP laminates", *Compos. Part B: Eng.*, **32**(4), 309-322. https://doi.org/10.1016/S1359-8368(01)00006-3.

Shaikh, F.U.A. and Taweel, M. (2015), "Compressive strength and failure behaviour of fibre reinforced concrete at elevated temperatures", *Adv. Concrete Constr.*, **3**(4), 283-293. http://dx.doi.org/10.12989/acc.2015.3.4.283.

Shen, R., Feng, L.Y. and Rong, K. (1991), "Assessment on mechanical property of rebar after elevated temperature (fire)", *Sichuan Build. Sci.*, **17**(2), 5-9.

Täljsten, B. and Elfgren, L. (2000), "Strengthening concrete beams for shear using CFRP-materials: evaluation of different application methods", *Compos. Part B: Eng.*, **31**(2), 87-96. https://doi.org/10.1016/S1359-8368(99)00077-3.

Van Coile, R. and Bisby, L. (2017), "Initial probabilistic studies into a deflection-based design format for concrete floors exposed to fire", *Procedia Eng.*, **210**, 488-495. https://doi.org/10.1016/j.proeng.2017.11.105.

Van Coile, R., Annerel, E., Caspeele, R. and Taerwe, L. (2013), "Full-probabilistic analysis of concrete beams during fire", *J. Struct. Fire Eng.*, **4**(3), 165-174.

Wang, G.Y., Liu, Q., Zhang, D.M. and Zhang, C. (2016), "A finite element model for post-fire seismic performance of steel reinforced concrete columns", *Eng. Mech.*, **33**(11), 183-192.

Weng, Y.H., Qian, K., Fu, F. and Fang, Q. (2020), "Numerical investigation on load redistribution capacity of flat slab substructures to resist progressive collapse", *J. Build. Eng.*, **29**, 101109. https://doi.org/10.1016/j.jobe.2019.101109.

Winful, D., Cashell, K.A., Afshan, S., Barner, A.M. and Pargeter, R.J. (2018), "Behaviour of high strength steel columns under fire conditions", *J. Constr. Steel Res.*, **150**, 392-404. https://doi.org/10.1016/j.jcsr.2018.06.008.

Won, D.H., Park, W.S., Jang, I.S., Han, S.H. and Han, T.H. (2014), "Fire resistance performance of steel composite hollow RC column with inner tube under ISO 834 standard fire", *Struct. Concrete*, **15**(4), 543-555. https://doi.org/10.1002/suco.201300067.

Wu, B. (2014), *The Mechanical Properties of Reinforced Concrete Structures after Fire*, Science Press, Beijing, China.

Xu, Y.L., Li, G.H. and Fan, C.J. (2014), "The finite element simulation analysis of reinforced concrete beams under high temperature based on ABAQUS", *Constr. Des. Project*, (6), 1-6.

Xu, Y.Y. and Wang, Q.F. (2010), "Research on residual strength of reinforced concrete columns after exposure to fire", *Eng. Mech.*, **27**(2), 84-89.

Yazdani, N., Beneberu, E. and Mohiuddin, A.H. (2018), "CFRP retrofit of concrete circular columns: Evaluation of design guidelines", *Compos. Struct.*, **202**, 458-464. https://doi.org/10.1016/j.compstruct.2018.02.066.

Yuan, J. (2017), "Reliability analysis of shear capacity of reinforced concrete beams", *J. Build. Struct.*, **38**(4), 109-128. https://doi.org/10.1680/jmacr.19.00367.

Yue, Q.R. (2000), "Present status of research and application of strengthening and repairing technology with carbon fiber reinforced plastics (CFRP) and its outlook in China", *Indus. Constr.*, **30**(10), 23-26.

Yue, Q.R., Chen, X.B. and Mu, H.Y. (1998), "New technology of carbon fibre reinforced plastics on strengthening & repairing concrete structures", *Indus. Constr.*, **28**(11), 1-5.

Zhang, B., Cullen, M. and Kilpatrick, T. (2014), "Fracture toughness of high performance concrete subjected to elevated temperatures Part 1 - The effects of heating temperatures and testing conditions (hot and cold)", *Adv. Concrete Constr.*, **2**(2), 145-162. http://dx.doi.org/10.12989/acc.2014.2.2.015.

Zhou, X.H., Tu, X., Chen, A.R. and Wang, Y.Q. (2019), "Numerical simulation approach for structural capacity of corroded reinforced concrete bridge", *Adv. Concrete Constr.*, **7**(1), 11-22. http://dx.doi.org/10.12989/acc.2019.7.1.011.